**Article:**
Cai, G, Tsavdaridis, KD, Si Larbi, A et al. (2021) A Simplified Design Approach for Predicting the Flexural Behavior of TRM-Strengthened RC Beams under Cyclic Loads. Construction and Building Materials, 285. 122799. ISSN: 0950-0618

https://doi.org/10.1016/j.conbuildmat.2021.122799

Accepted by Construction and Building Materials

2021.02.21

# A simplified design approach for predicting the flexural behavior of TRM-strengthened RC beams under cyclic loads

**Gaochuang Cai[1*], Konstantinos Daniel Tsavdaridis[2]*, Amir Si Larbi[1], Phil Purnell[2]**

[1] Univ Lyon, Ecole Nationale d'Ingénieurs de Saint-Etienne (ENISE), Laboratoire de Tribologie et de Dynamique des Systèmes (LTDS), UMR 5513, 58 Rue Jean Parot, 42023 Saint-Etienne Cedex 2, France.

[2] School of Civil Engineering, University of Leeds, Woodhouse Lane, Leeds LS2 9JT, UK.

*Corresponding author*:

G. Cai, gaochuang.cai@enise.fr;

K. D. Tsavdaridis, K.Tsavdaridis@leeds.ac.uk;

**Abstract**

This paper proposes a simplified design approach to predict the flexural behavior of reinforced concrete (RC) beams strengthened by high-performance textile reinforced mortar (TRM) under cyclic loads. Based on the experimental results, the effect of main factors on the beams, and the effectiveness and reliability of TRM strengthening layer under cyclic loads were examined as per ACI 437 method. The reinforcement ratio of the original RC beams, the textile reinforcement ratio of TRM layer, and the interface bond between the original beam and TRM layer all have a significant influence on the flexural behavior and failure modes of TRM-strengthened beams. The simplified models based on the *fib* model and Architectural Institute of Japan (AIJ) standard were suggested to predict the flexural capacity of the strengthened beams, which were used to evaluate the flexural curve of the beams together using simplified calculation models of the deflection capacities of the RC beams. The results verified that the simplified capacity curve model presented good accuracy to evaluate the TRM-strengthened RC beams.

**Keywords:** Textile reinforced mortar; Flexural strengthening; Strengthening reliability; Flexural capacity curve; Cyclic flexural loads

## 1. Introduction

Reinforced concrete (RC) is still the most commonly used and practical material for civil and infrastructure engineering, due to its cost-efficiency and strength as well as the easy acquiring of materials for producing concrete. However, existing RC structures may require strengthening or retrofitting to extend their lifespan or to meet their serviceability at updated external conditions. To be specific, these strengthening and retrofitting may be needed for : (1) the deterioration of structural performance due to concrete aging, (2) the changes in the use purpose of the structures usually accompanied by changes in load conditions, and (3) design codes were updated for safety and economic considerations. Consequently, the strengthening and repairing of the RC structures are inevitable in some cases. Until now, a large number of experimental and numerical investigations have been conducted for seeking suitable and reliable structural strengthening and retrofitting methods, most of which usually recommended applying advanced composite materials such as fiber-reinforced polymer (FRP) materials for their high strength-weight ratio[1-8].

The widely-used methods of strengthening of RC structures at the early stage of previous research generally include strengthening with high-performance cementitious materials such as external high strength mortar repairing layer [9], or high strength concrete layer [10] and high performance engineered cementitious composites [11-16]. However, all the methods usually increase the self-weight of the original RC structure, affecting significantly utilizing the space of structures. Moreover, the durability issues of strengthened or repaired external layers also affect significantly the safety of the structures in the future. Using steel plates or external strengthening members [17] to strengthen RC structures may also incur the same problems on self-weight and durability (see Fig.1) of the structures. With the development of high strength and high durability materials such as FRP grids [18, 19], the durability issues of the elements using such strengthening materials mentioned above could be improved, however, the low formability of the strengthening layers may restrict the above methods to be used in complex structures (the structural elements with multi-shapes). A series of experimental and numerical studies have been conducted to understand the performance of FRP strengthened RC structures and optimize design methods [4]. However, some drawbacks still have been observed with the use of FRP sheets, which are mainly associated with the use of epoxy resins [20, 21], as well as the surface vulnerability of the FRP sheet which also could easy to lead a potential safety issue.

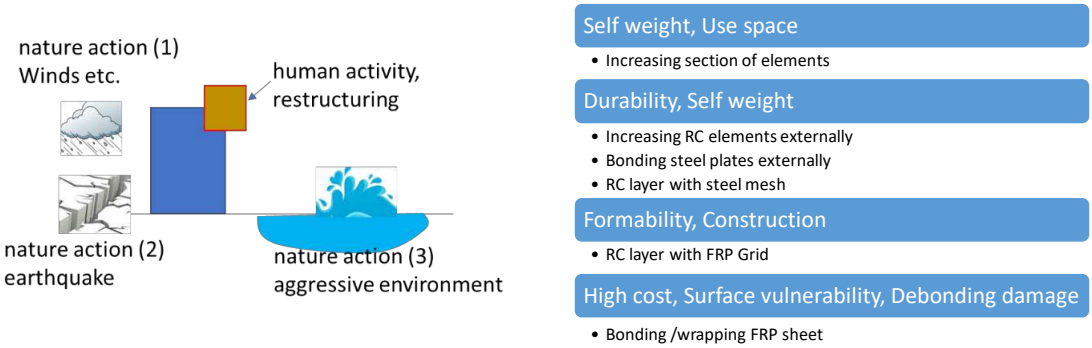


Fig.1 Deterioration of RC structures and main issues of existing strengthening methods

Numerous researchers [22-29] developed alternative solutions for repairing and strengthening damaged old RC structures using some high-performance cementitious layers containing innovative reinforcements and materials. One representative of these methods is textile-reinforced concrete or mortar (TRC or TRM) which is a lightweight, high performance, and excellently durable material and can form a better interface bond with the original concrete surface comparing with FRP sheet materials. A TRC/TRM strengthening layer consists of one or multilayer textile fabrics bonded with high-performance concretes or mortars. The effectiveness of TRC/TRM strengthening layers on original structures under monotonic loads also has been researched fully [20-23], [30-34, 35-41]. The main findings of the TRM-strengthening technologies have been reviewed and summarized recently [42,43] and several design models [35-37, 39-41] and FEA approach [38] also were proposed based on the experimental and numerical studies in those studies. However, most of the studies focused on the structural behaviors of the beams under monotonic shear or flexural loads [20,21,30-35], and the design model of TRM- or TRC-strengthened RC beams is very limited. Therefore, the reliability of this strengthening method under cyclic loads should be examined, to understand the strengthening of existing RC structures under cyclic loads and develop the related design approaches.

Therefore, as a preliminary study, this paper aims to preliminarily investigate the flexural performance of RC beams repaired by TRM layer under cyclic loads and to propose a simplified method for predicting the flexural behavior of TRM strengthened beams. The strengthening effectiveness and reliability of the TRM-strengthening method are examined by analyzing the cyclic load-deflection curves, failure modes, and ductility performance of the beams in detail.

## 2. Experimental program

As described in the previous studies reported in the literature [44,45], a four-point flexural test was performed to study the flexural behavior of RC beams designed as per current Eurocode 2 [46]. The detailed information of the beams is depicted in Fig.2 and Table.1, including the dimensions and reinforcement arrangement of the beams. Beams CB1 was used as a control beam (without strengthening) and was tested under monotonic load. Beam CB2, without strengthening layer as well, was tested under cyclic load, while TB1 and TB2 were strengthened with TRM (different mortar strength) but without a pre-cracking process. Many previous studies [47-50] applied a pre-cracking process to simulate the damages of original RC structures before strengthening in their experimental work. Therefore, another two strengthened beams (PTB1, PTB2) were pre-cracked in 40% of reference flexural load ($P_{re}$) of the beams before strengthening the beams by TRM layer. The two beams (PTB1,2) used the same concrete as the original RC beam and the same TRM layer as the beam TB1 or TB2, but they used different layers of textile fiber mech in TRM layer. The reference load was applied corresponded to the maximum allowed deflection of the beams for serviceability limit states according to the Eurocode 2 [46], i.e., when the midspan deflection of RC beam reached 1/250 of beam span. Before performing the strengthening process of TRM layer in the test beams, several pretreatments of concrete substrate were conducted, mainly including surface roughening, removing dust and moistening the surface appropriately.

Table.1 Specimen details

| Specimens # | Beam sectional width x depth (mm) | Pre-load ratio (% of $P_{re}$) | Longitudinal reinforcement | Steel stirrups | Compressive strength of concrete /mortar (MPa) | Applied Loading type | The number of layers of fiber mesh in TRM |
|---|---|---|---|---|---|---|---|
| CB1 | 150x250 | 0 | 3D12+2D10 | Steel R8, spacing 170 mm | 39.40/- | Monotonic | 0 |
| CB2 | | 0 | | | 39.40/- | Cyclic | 0 |
| TB1 | | 0 | | | 35.96/73 | Cyclic | 1 |
| TB2 | | 0 | | | 35.96/80 | Cyclic | 1 |
| PTB1 | | 40 | | | 41.09/59 | Cyclic | 1 |
| PTB2 | | 40 | | | 41.09/56 | Cyclic | 2 |

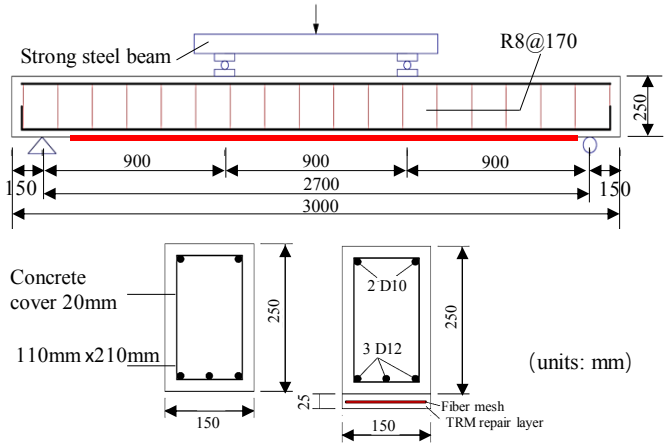


Fig.2 Testing method, dimensions and reinforcement arrangement of specimens

### 2.1 Properties of materials

C40 concrete was used for all the tested beams in the current study. The related mechanical tests of the used materials were performed referring to the standard tests of three standard cylinder specimens (diameter 150mm, height 300mm) cured in a standard curing room (relative humidity of 95%, the temperature of 18 $^{o}$C-22$^{o}$C). The mean modulus of elasticity of the concrete was 34.26GPa. S500 standard steel rebars were used as longitudinal (tensile and compressive sides) and transverse reinforcements in the beams, with a yield strength of 570MPa (deviation of 13MPa). A high-performance mortar was applied for producing TRM strengthening layers, which used fly ash, micro silica, and fine-grained sand (0.2mm-0.6mm). The tested compressive strengths of the mortars used in each beam are listed in Table 1. The used textile fiber mesh was provided by FORMAX company and was made of carbon fiber, using 50 thousand (50k) of filaments per roving, a density of 260g per square meter, and bi-directional textile (0/90 degree). Fig.3 depicts the details of the textile fabric mesh including dimensions and main mechanical properties, which were provided by the supplier with a certificate guarantee. For strengthening the beams, the repair surface of the concrete at the tensile zone of the beams was firstly wetted, and then the first layer of mortar was sprayed. Subsequently, the fabric mesh was laid to contact with the mortar, and then the rest of the mortar was cast to cover the fabric mesh. The total thickness of the strengthening TRM layer was 25mm, as shown in Fig.2.

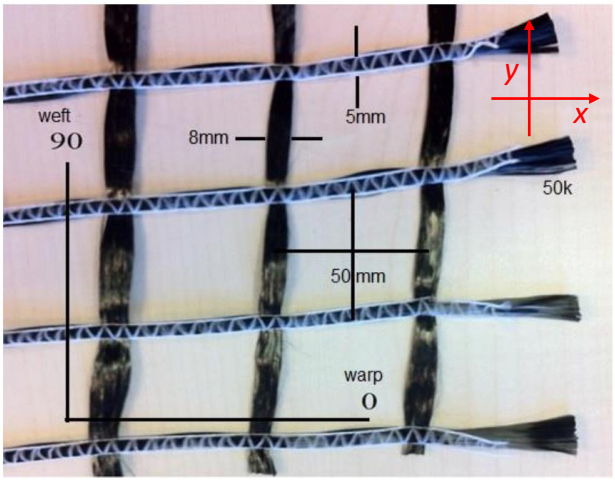


| Main properties of textile fiber mesh | | |
|---|---|---|
| Filament diameter | $\mu m$ | 7.0 |
| Number of filaments | $k$ | 50 |
| Fabric weight | $g/m^2$ | 150 |
| Mesh spacing (x & y) | $mm$ | 50 |
| Mesh clear spacing x (y) | $mm$ | 42(45) |
| Tensile strength ($f_f$) | $MPa$ | 4000 |
| Modulus ($E_f$) | $GPa$ | 235 |

Fig.3 Details of textile fabric mesh used in TRM layers

### 2.2 Loading procedure and measurement

All beam specimens were tested cyclic flexural load except for the control beam was tested under static monotonic for comparative study. The loading rate of all beams was set as 5kN/min. The loading method of the cyclic tests was referred to ACI 437.1R [51] and FEMA 461[52] codes, and previous studies [53-58]. According to ACI 437.1R [51], a closed-loop test was commonly used to confirm the behavior of concrete beams under cyclic loads. This cyclic load was based on concentrated loads in a quasi-static method by producing at least six loading/unloading cycles. The detailed processes of loading-unloading cycles are shown in Fig.4, in which the first two cycles (Cycles *A* and *B*) were applied as 10kN (1$^{st}$ $P_{ref}$) while the cycles *C* and *D* were applied for 20 kN (2$^{nd}$ $P_{ref}$) in the current study. The increment rate of the reference load $P_{ref}$ was 10kN in the rest procedures of the load. The tests were stopped when the failure state of the test beams was confirmed. The deflections of the beams were measured by several Linear Variable Differential Transformers (LVDTs) placed at the mid-span, and the right and left sides with 150 mm away from the two supports. Two LVDTs were placed at the ends of the beams to check the potential movement of the beams in the horizontal direction. Two wire-type strain gauges were placed on the middle longitudinal steel reinforcement and five wire-type strain gauges for concrete were placed on the interface zone between the old concrete surface of the original beams and TRM layer, in the strengthened beams. These gauges to check the location of the neutral axis of the beams during the loading. For the pre-cracked RC beams (PTB1 and PTB2), a pre-loading procedure was conducted and stopped when the mid-span deflection of the beams reached 6.0mm, i.e., 50% of 1/250 of maximum allowed deflection of the beam at serviceability limit states

as per Eurocode [46]. According to the test, the maximum load applied in the pre-cracking tests was 33.2kN for both beams PTB1 and PTB2. During the pre-cracking test of PTB1 beam, the first crack load was 15kN, and the crack was continuously extended up to 33kN, 40% of the reference load described before. For Specimen PTB2, the first crack was observed when the load reached 20kN, and then developed until 40% of the reference load (33kN).

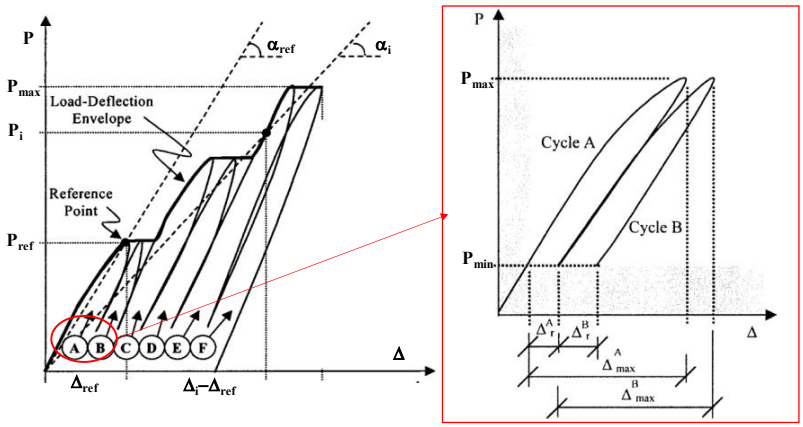


Fig.4 Applied cyclic loading in the study as per ACI 437.1R (ACI 2007)

## 3 Test results and discussion

### 3.1. General observations

Fig.5 presents the damage of several representative tested beams. In the tests, the following observations were summarized as (1) CB1 beams experienced a typical evolution of flexural cracks and damage and finally presented a flexural failure mode; (2) the de-bonding damage of TRM layer still was observed in the strengthened beams, the other two main damages were the crushing of concrete in compression zone and fracture of TRM layer in the beams; (3) the cracking of the layer was sufficiently propagated before the fracture of TRM layer; (4) the pre-cracking of RC beams does not significantly affect the final failure mode and damages of the beams, however, the de-bonding was postponed in pre-cracked specimens PTB1 and PTB2, which made the concrete cracks were fully developed.

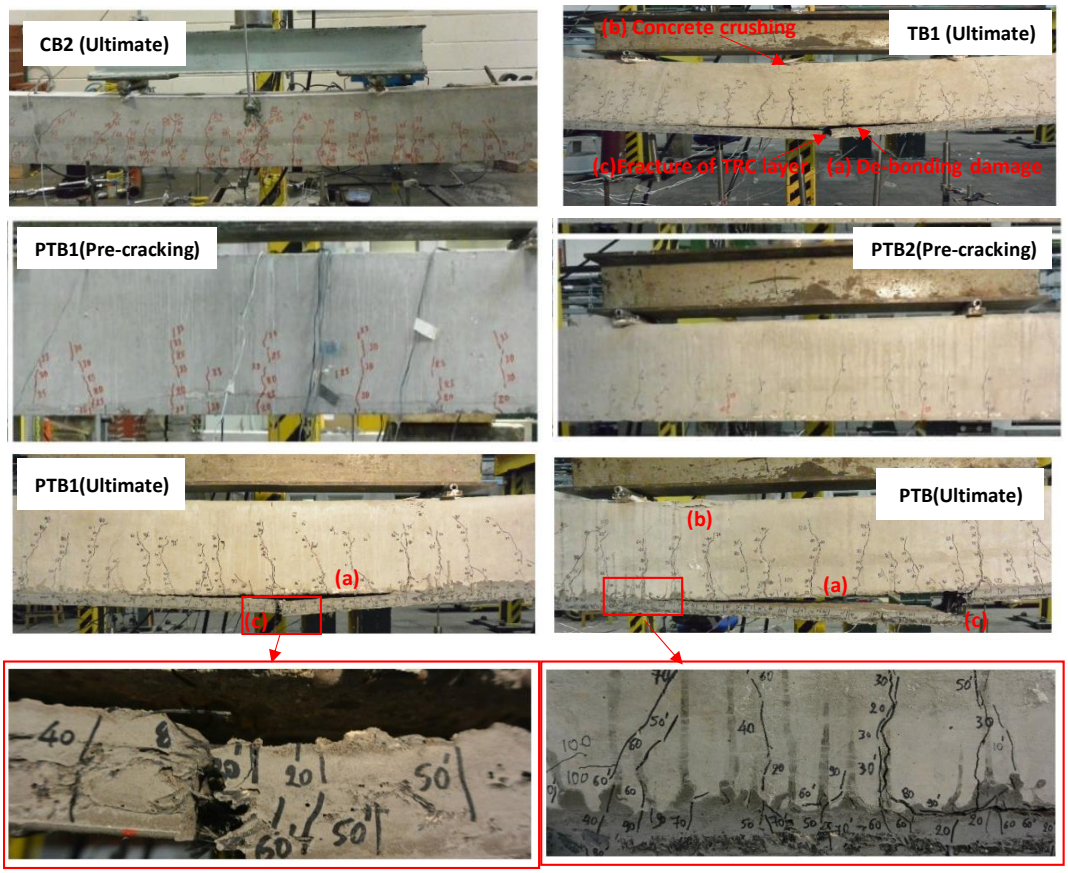


Fig.5 Main damage and failure of tested beams

### 3.2. **Load-deflection behaviors of the beams**

As shown in Fig.6 (a), although the cyclic load usually affects disadvantageously the stiffness of RC beams, the load-deflection curve of the beam (CB2) under cyclic load presents a higher initial stiffness than that of Beam CB1. At the early stage, the high initial stiffness provides a higher elastic restoring for the beam at the early stage of unloading, which means the entire flexural deformation and damage accumulation of the beam can be reduced slightly. However, at the later stage of the cyclic loading, the damage and cracking development of the beam caused by cyclic loads increased until the final failure state of the beam was reached, which is partly due to the large damage and deformation of the beam. However, the ultimate deformation and peak load of the beam under monotonic load were larger than those of the beam under cyclic load, i.e., the maximum load and deflection of Beams CB1 and CB2 were 84kN and 80kN, and 38 mm and 35 mm, respectively. This also implied that the early-age accumulated damage accelerated the final failure of the TRM strengthened beam. Besides, the final unloading path of the beam CB2 was similar to

that of the beam CB1 in terms of peak load and the slope of the unloading path. A similar phenomenon was reported in FRP strengthened RC beams [59]. Fig.6 (b) shows the effects of the TRM strengthening layer on the beams without the pre-cracking process, in terms of initial stiffness, peak load, and the maximum deformation of the beams. The peak loads and the midspan deflections corresponding to the peak loads of the two strengthened beams were similar, as well as their deformation abilities both were higher than those of the beams CB1 and CB2. However, the difference between the ultimate deflection of the two beams TB1 and TB2 was quite large. The results of the pre-cracked strengthened beams with TRM layer are plotted in Fig.6 (c), demonstrating that similar behavior was observed. However, comparing with the results in the beams TB1 and TB2 plotted in Fig. 6 (b), the TRM strengthening effectiveness and ultimate deformation of the beams with the pre-cracking process were higher. The difference between the specimens PTB1 and PTB2 can be explained by the fact that PTB2 specimen used two layers of textile fabric meshes in the TRM layer. As shown in Fig.6 (d), regardless of the pre-cracking of the beams, the strengthening effectiveness of TRM layer was verified in terms of peak load and deformation ability. When using the pre-cracking process, a better interface bond could be provided between the original concrete surface and TRM layer, which contributes to the strengthening effectiveness of TRM layer. Also, as shown in Fig.6 (d), the TRM with two layers of textile meshes provides the best strengthening to original beams, although the compressive strength of the mortar in the TRM layer applied in the beam PTB2 was slightly smaller than others. This implies that the TRM layer with more layers of fabric meshes can provide a higher flexural resistance and deformation ability. According to this, it may be concluded that the use amount of textile fabric mesh in TRM layer is a key parameter for the design of the flexural capacity of TRM strengthened RC beams. Table.2 lists the main feature points of the load-deflection curves of the beams.

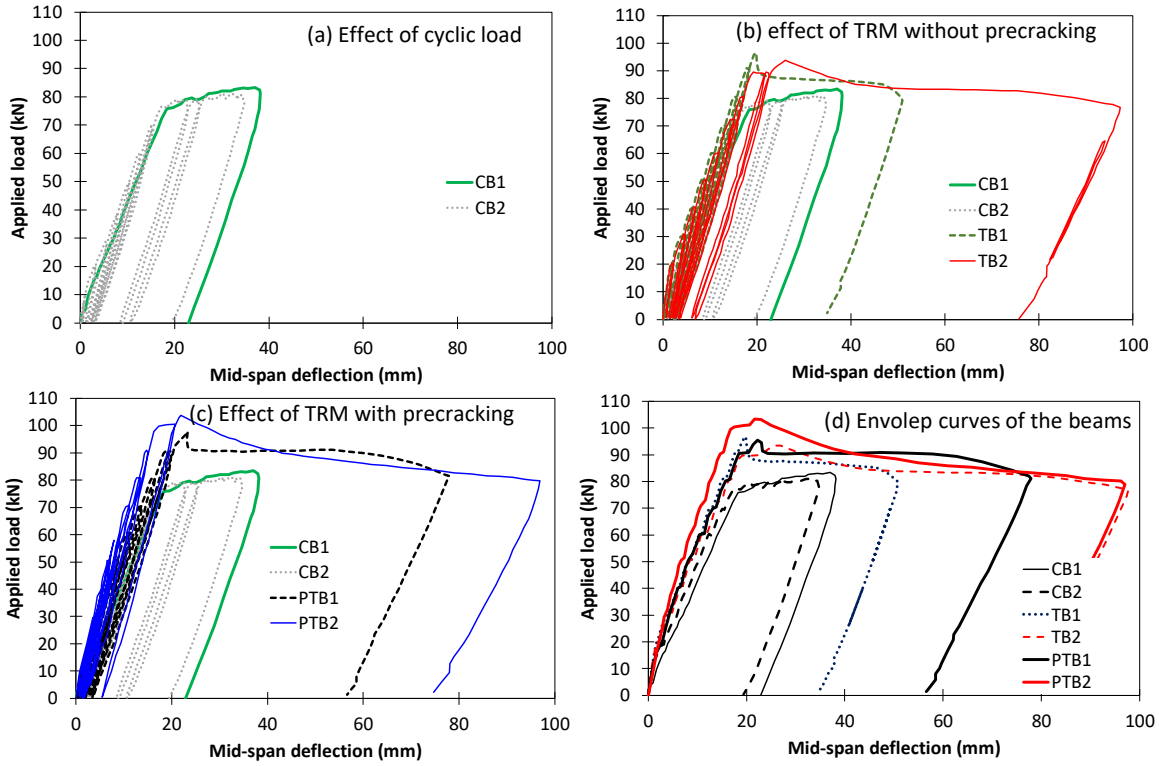


Fig.6 Load-midspan deflection behavior of tested beams

Table.2 Summary on results of tested specimens

| # | Fabric mesh layer | Fc (MPa) | Yield load $P_y$ (kN) | Peak load $P_m$ (kN) | Moment $M_{max}$ kNm | Yield midspan deflection $\Delta_y$ (mm) | Peak midspan deflection $\Delta_m$ (mm) | Ultimate midspan deflection $\Delta_u$ (mm) | Peak Ductility $\delta_m$ | Ultimate Ductility $\delta_u$ |
|---|---|---|---|---|---|---|---|---|---|---|
| CB1 | 0.00 | 39.40 | 75.69 | 83.69 | 37.66 | 18.50 | 37.90 | 38.30 | 2.05 | 2.07 |
| CB2 | 0.00 | 39.40 | 75.90 | 81.23 | 36.55 | 17.50 | 34.80 | 34.30 | 1.99 | 1.96 |
| TB1 | 1.00 | 35.96 | 79.30 | 93.49 | 42.07 | 17.10 | 19.20 | 97.02 | 1.12 | 5.67 |
| TB2 | 1.00 | 35.96 | 78.60 | 96.21 | 43.30 | 19.87 | 26.00 | 50.82 | 1.31 | 2.56 |
| PTB1 | 1.00 | 41.09 | 81.10 | 97.47 | 43.86 | 18.10 | 22.50 | 77.65 | 1.24 | 4.29 |
| PTB2 | 2.00 | 41.09 | 84.20 | 103.53 | 46.59 | 18.50 | 23.76 | 96.67 | 1.28 | 5.23 |

$F_c$ is the compressive strength of concrete, in MPa; $M_{max}$ is the peak moment of the beams, in kN.m; $\Delta_y$, $\Delta_m$, and $\Delta_u$ are the midspan deflections of the beams corresponding to their yield load ($P_y$), peak load ($P_m$) and ultimate load (taken as $0.85P_m$), in mm. $\delta_m$ and $\delta_u$ are the peak and ultimate ductility of the beams corresponding to peak load and ultimate load, respectively.

### 3.3. Deformation of the tested beams

The deformation capacity of RC beams is one of the important factors affecting the safety of RC structures.

Table 2 summarizes the measured midspan deflection of the beams and calculative displacement ductility

corresponding to the peak load and ultimate load of the beams. Test results verified that the mid-span deflections and ductility of the RC beams at the ultimate state increased with the number of layers of fabric mesh in TRM layer, which attributes to that the more fabric meshes provide more effective tensile resistance to the strengthened layer at large deformation stage. However, the effect of the number of mesh layers on the yield deflection of the strengthened beams was slight, which can be explained that only small damages and deformation occur in the TRM layer before the yielding of the beams. Therefore, the yielding deflection still was dependent on the longitudinal steel reinforcements of the original beams, which led to the yield deflections of the beams are almost the same for the same longitudinal reinforcement ratio was used in the beams.

### 3.4. Evolution of secant stiffness of the test beams

Fig.7 presents the evolution of the secant stiffness of the beams with their applied flexural loads. It is found that the initial secant stiffness of the beams was affected by the pre-cracking process of the original beam, regardless of how many layers of fabric mesh were used in TRM layer. The TRM–strengthened beams PTB1 and PTB2 presented a similar stiffness, about 20000 kN/m, while the initial stiffnesses of the beam CB2, and those of the beams TB1 and TB2 without the pre-cracking process were approximately 35000 kN/m. Up to the applied load of 30kN, the secant stiffness of all beams decreased significantly to a similar level, which only about 5000kN/m. Besides, the secant stiffness of the beam PTB2 with pre-cracking was just slightly larger than th0se of other beams, after the loading of 30kN. This indicates that even if the pre-cracking process reduced the stiffness of the strengthened beams, however, the beams can achieve a slightly higher stiffness at a large deformation stage when more layers of textile meshes are used in strengthening TRM layer.

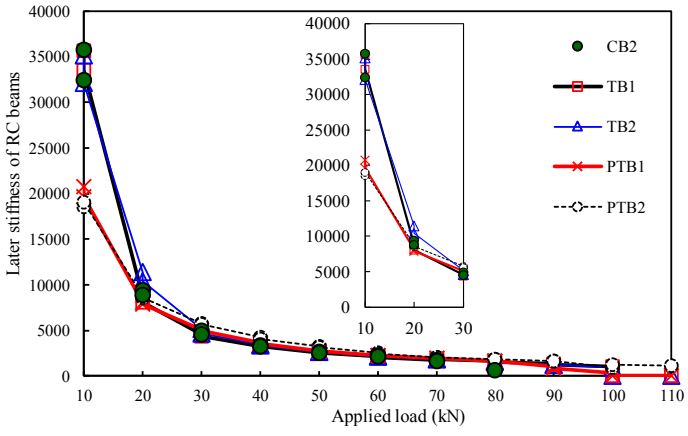


Fig.7 Evolution of secant stiffness of the beams

## 4 Discussion of effectiveness and reliability of TRM strengthening method

### *4.1 Strengthening effectiveness of TRM layer on RC beams*

In this section, the strengthening effectiveness of TRM layer on the beams under cyclic flexural loads and the position of the neutral axis of beams are discussed. Fig.8 (a) demonstrates that a stable increase could be available in the flexural capacity of the TRM-strengthened beams by increasing the number of layers of textile fabric meshes in the TRM layer, which proved the effectiveness of the TRM layer in the beams. Comparing with the control beam, the applied load capacity of the strengthened beam all were higher than those of the control beam by about 30%. However, this increase in load-carrying capacity was affected by the addition of the pre-cracking process of the original beams. Among all strengthened beams, the yield and peak loads of the beams with pre-cracking both higher than those of the beams without the process, regardless of the usage amount of fabric textile mesh. For the beams with the pre-cracking process, the peak load of the beam with 2 layers of textile fabric mesh was higher than those of the beam specimens using one mesh layer by 10%. However, this increase of the beams without the pre-cracking process could be due to the increase of the compressive strength of the mortar in the TRM layer, as listed in Table 2. Considering this, Fig.8 (b) demonstrates the ratio of applied peak load to the compressive strength of mortar in TRM layers, in which the beneficial effect of the number of layers of textile fabric mesh on the beams was proved. The yield loads of the beams presented a similar trend with the number of layers of fabric mesh in the TRM layer when taking off the effect of the compressive strength of concrete in the original beams.

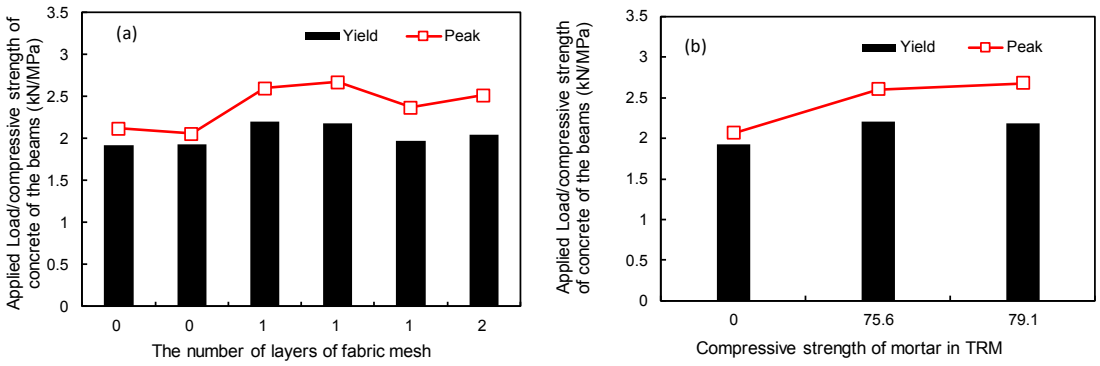


Fig.8 Flexural capacity of TRM strengthened RC beams with different conditions

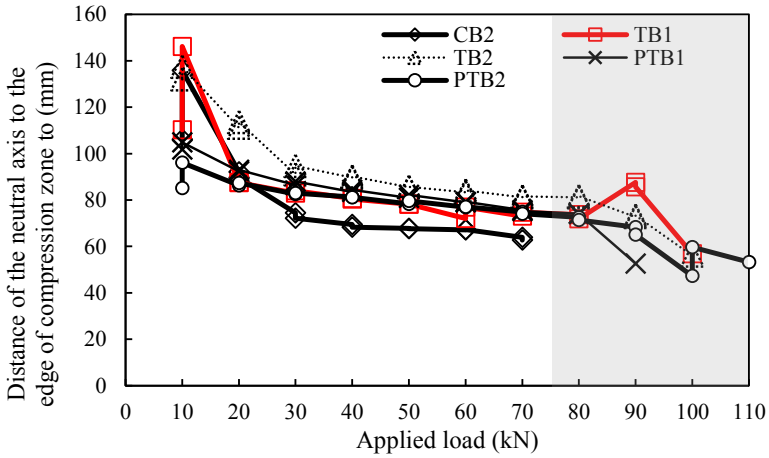


Fig.9 Development of the distance of neutral axis to the edge of the compression zone of the beams

In addition, the development of the distance from the neutral axis of the beams to the compression edge of the beams is presented in Fig.9. Results show that the localization of the neutral axis of the beams decreased as the applied load of the beams. Comparing with the beam CB2, other beams presented a higher distance of the neutral axis, meaning the TRM strengthening layer can effectively resist the cracking proliferation of the beams. However, the decrease trends of the distance of all beams with applied loading were similar, implying that TRM layer could work together well with the original beams to resist the flexural loads. Besides, the distances of the neutral axis of the beams PTB1 and PTB2 both were decreased with a similar slope at the large deformation stage, from 100mm to about 60mm, despite that the different layers of textile fabric meshes were used. This may be caused by the debonding failure of the beams at the stage. The results of the beams CB2, PTB1 and TB2 were also similar, however, the distances of the beams largely degraded starting from 30 kN. Between 30kN and 70kN, the degradation slope of the neutral axis distance of all beams was similar, which was because the main damage and cracking development of the beams occurred in the loading zone such as debonding failure and the large deformation of TRM layer. After the flexural load was increased at a certain level during cyclic loads, the effective height of the compression zone of the beams was reduced stable until the beams reached the failure status. The effective area of the compression zone of the beam PTB2 was the smallest, meaning that the strengthening effectiveness of the TRM layer with two-layers meshes was the largest, which was validated by the experimental damage and deformation observations described before.

### *4.2 Reliability of the TRM strengthening method*

According to the assessment method proposed by ACI committee 437 [51], the reliability of concrete beams under cyclic loading can be examined by discussing (1) the repeatability of the deflection of beams, (2) the

deviation from linearity, and (3) the permanency of the beams. The repeatability of the element deflection was defined as Eq.(1), which was the difference ratio of maximum deflection to residual deflection measured during the first two loading cycles, which should be greater than 95%. The deviation from linearity was defined as the parameter for measuring the non-linear behavior of the elements under cyclic loads, which should be less than 25%. The three factors are given as follows:

$$Repeatability = \frac{\Delta_{max}^{B} - \Delta_{r}^{B}}{\Delta_{max}^{A} - \Delta_{r}^{A}} \times 100\% \quad (1)$$

$$Deviation\ from\ Linearity_i = 100\% - \frac{\tan(a_i)}{tan(a_{ref})} \times 100\% \quad (2)$$

$$Permanency = \frac{\Delta_{r}^{B}}{\Delta_{max}^{B}} \times 100\% \quad (3)$$

In the equations, $\Delta_{max}^{A}$ and $\Delta_{max}^{B}$ are the maximum deflection in Cycles *A* and *B* under the applied load of $P_{max}$, $\Delta_{r}^{A}$ and $\Delta_{r}^{B}$ is the residual deflection at Cycles *A* and *B* under the applied load of $P_{min}$. The ACI 437 [51] suggested the same procedure can be used to measure this ratio for Cycles *C* and *D*. The $tan(a_{ref})$ and $tan(a_i)$ are the slope of a reference secant line and the slope of the secant line at Point *i* in the load-deflection envelope curves. The permanency of elements is the amount of permanent change displayed by any structural response parameter during the second cycle of the two cyclic loads, which should be not greater than 10%. By comparing with the factors of the TRM-strengthened beams studied in the current study, the strengthening effectiveness of the TRM strengthening method under cyclic loads was evaluated.

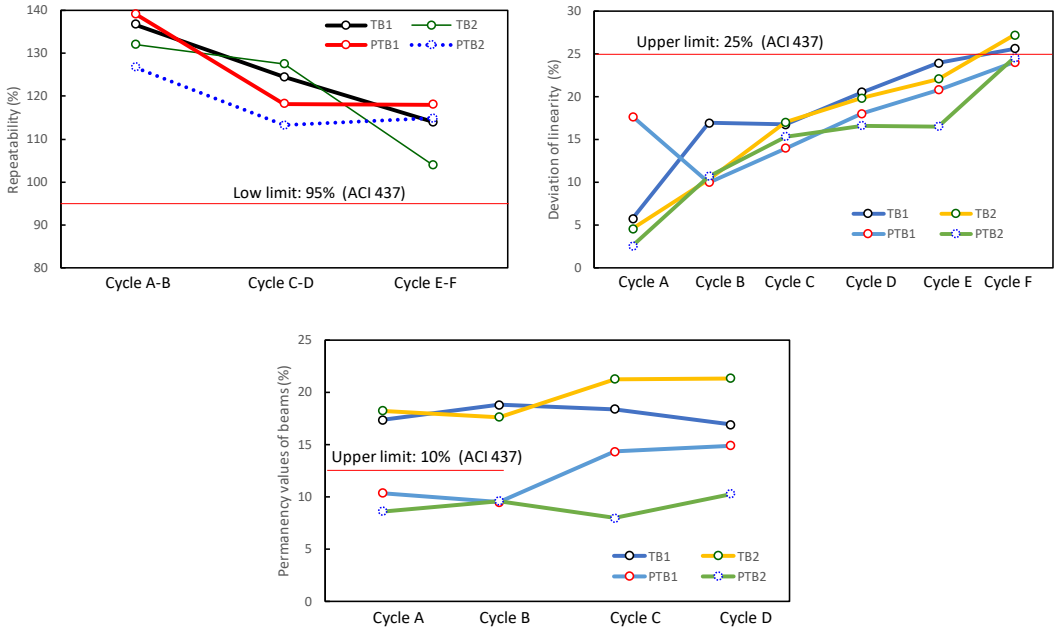


Fig.10 Reliability of TRM strengthening method under cyclic loads as per ACI 437 [51]

Fig.10 shows the experimental results of the repeatability, the deviation from linearity and the permanency of the strengthened RC beams. Results show that the repeatability of all beams was higher than 95%, meaning the beams could satisfy strengthening requirements for cyclic loads as per the ACI 437 [51]. On the other hand, for the beams without the pre-cracking process, the values of the deviation of linearity of the beams TB1 and TB2 were higher than 25%, the critical level proposed by ACI 437 [51] at the sixth cycle. Based on this, it was understood that the pre-cracking affected the non-linear behavior of the TRM-strengthened beams under cyclic loads at the large deflection stage for the different interface bond behavior. Besides, the results of the permanency of the beams also supported the descriptions about the beams without the pre-cracking process. The permanency of pre-cracked beams PTB1 and PTB2 was less than 10% suggested by ACI 437 for a better interface bond was provided between the original beam and TRM layer, while the levels of the other beams all were greater than 16% in loading cycles *A* and *B*.

### *4.3 Damages and failure modes of TRM strengthened beams*

The main characteristics of the load-deflection curves of the tested beams are shown in Fig.11. Based on the analyses described before by Cai *et al.*[44], similar to the RC beams strengthened by FRP sheet, the key factors affecting the load-deflection curves of the beams include the ratio of longitudinal reinforcement of original beams, the mechanical properties of TRM layer, and the concrete-TRM interface bond. It was well understood that the reinforcement of original beam with limited damage and corrosion is a very important factor for the structural behavior of RC beams [60]. In the current study, before TRM strengthening layer was applied, the beams were not subjected to any external damage and corrosion, and there is little influence from the pre-cracking process. Therefore, all beams experienced a flexural failure mode (e.g, Case *f* or *e*). The reinforcements in the beams developed their deformation continuously and many typical flexural cracks were observed. When using a high-performance TRM layer providing a perfect interface bond with the beams, the load-carrying capacity and stiffness of the beams can be improved significantly up to the large deflection stage, and present a deflection-hardening behavior, as Case *a* shown in Fig.11. However, in this case, if the interface bond is slightly small, during the deformation hardening stage, the load-carrying capacity usually decreases from its peak load which may be attributed to the de-bonding failure at the large deformation stage (Cases *b* or *c*). The declining slope of the flexural capacity curve is up to the properties of the interface bond and TRM layer. The failure mode of the specimen PTB2 with two layers of textile meshes belonged to this mode. However, if the TRM layer and its interface bond with the surface of the beam are both slightly smaller, the peak load of the beam usually occurs earlier and the load capacity of the beam also may decrease more sharply compared with the cases mentioned above. Comparing with all

aforementioned cases, when a moderated bond and TRM layer are applied, the load-deflection curve of TRM-strengthened beams usually presents a stable and gentle development (Case *c*). The literature[61] has also reported similar observations and analyses. Fig.11 describes some typical damages and deformations of TRM-strengthened RC beams under cyclic flexural loads based on the study.

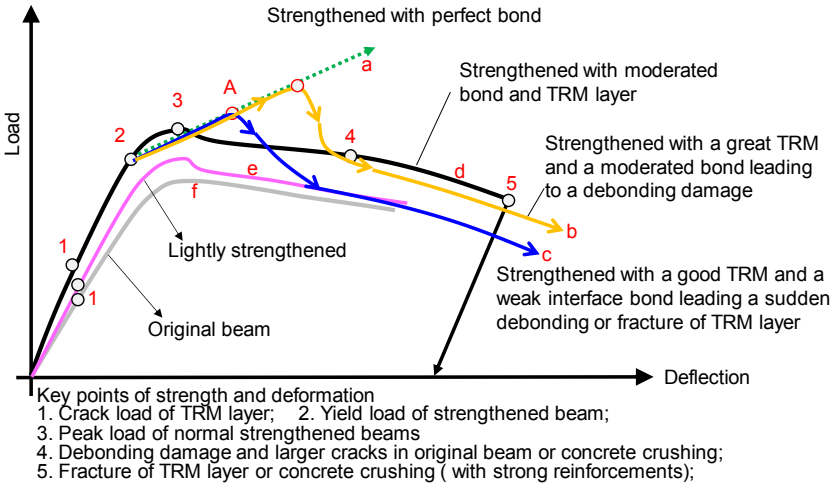


Fig.11 Main characteristics and failure modes of TRM-strengthened RC beams

## *5 Flexural design of TRM-strengthened RC beams*

In the past twenty years, many studies have been conducted to analyze the design capacity of RC beams strengthened by TRM or Textile reinforced concrete (TRC) layer under monotonic loading such as monotonic shear load [20, 35] and flexural load [21]. Several calculation models also were proposed based on the experimental and numerical studies in those studies, including shear models [35-37], and flexural models [39,40] and analysis method [42] FEA approach[38]. However, as described before, the design model of TRM- or TRC-strengthened RC beams is very limited, as far as the authors know.

### *(1) The theoretical flexural capacity of TRM-strengthened RC beams*

Based on the test results described before and referring to Section 4.4.1 in *fib* Bulletin 52 [62], the following assumptions were used for calculating the theoretical flexural capacity of TRM-strengthened RC beams,

(i) Sections plane in the unloaded state remain plane during loading;

(ii) Bonded reinforcement undergoes the same strain increments as the adjacent concrete;

(iii) The maximum strain of the concrete is equal to the value at the ultimate limit state, $\varepsilon_{cu}$;

(iv) The tensile stress in concrete is neglected.

According to the literature [62], the modeling of the internal forces resisting flexure behavior was used. Assuming the longitudinal steel reinforcements in the original beam yielded and the textile fabric mesh layer reach *k* times its yield strength in the TRM strengthening layer, therefore, the equilibrium condition in the longitudinal direction is given as:

$$f_{cd1} \cdot b \cdot x = A_{s1} f_{yd1} + A_{s,T} k f_{y,T,e} \quad (4)$$

$$x = \frac{A_{s1} f_{yd1} + A_{s,T} k f_{y,T,e}}{f_{cd1} \cdot b} \leq 0.5\mathrm{d} \quad (5)$$

$$f_{cd1} = 0.85 \left[1 - \frac{f_{ck}}{250}\right] f_{cd} \quad (6)$$

$$\varepsilon_{cu} = 0.004 - 0.002 \frac{f_{ck}}{100} \quad (7)$$

where *k* is the assumed reduction ratio of the maximum strain to the yield strain of textile mesh layers. $f_{ck}$ is the characteristic value of concrete strength, i.e., the 5% fractile value of the compressive strength of standard concrete cylinder specimen (diameter/height=150mm/300mm), which could be calculated as $f_{cm}$-$\Delta f$ as per the *fib* Bulletin 51 [63]. $f_{cm}$ is the mean measured compressive strength of concrete and $\Delta f$ was assumed as a constant value of 8MPa according to the MC2010 [64] in the current paper. $f_{cd}$ is the design compressive strength of concrete taken as $f_{ck}$/1.5 considering a safety factor of 1.5 in *fib* Bulletin 52[62]. $f_{cd1}$ is the average design strength of concrete in the uncracked compression zone. According to Section 4.4.1 in *fib* Bulletin 52[62], a constant $\varepsilon_{cu}$ of 0.0035 could be used in Eq. (7) without creating any major problems.

Besides, the cross-sectional area of the textile fabric meshes in the beams, $A_{s,T}$, was suggested to consider the effect of filament bundles at the different direction on longitudinal textile fiber bundles in TRM layer. Therefore, in the study, $A_{s,T}$ was calculated by:

$$\mathrm{A}_{s,T} = \gamma \cdot n \cdot A_{fli} \quad (8)$$

where, $A_{fli}$ is the area of each filament bundle in fabric mesh; $n$ is the number of filament bundles at the longitudinal direction in strengthening cross-section; $\gamma$ is an enhancement factor considering the effect of the filament bundles at the different directions, ranging from 1.0 to 1.5 depending on the mesh size of the textile fabric layer, which was taken as 1.3 in the study.

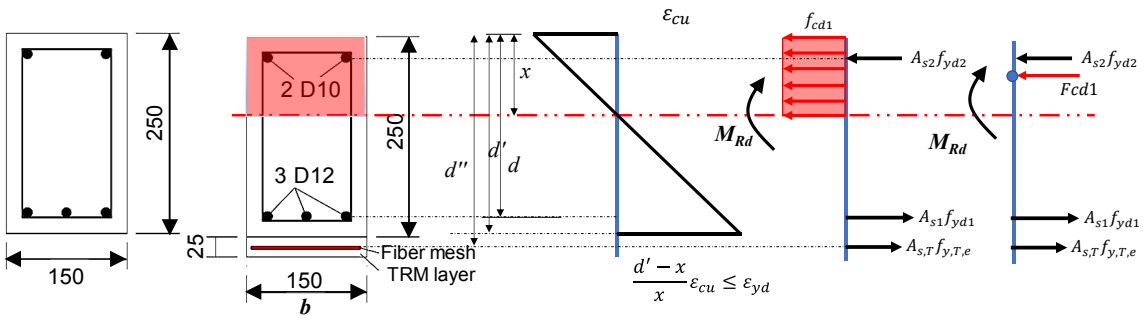


Fig.12 Sectional analysis of TRM-strengthened RC beams under flexural loads

As shown in Fig.12, taking the moments at the center of the compression zone as the design resistance moment $M_{RD}$, therefore, the flexural capacity of the TRM-strengthened RC beams can be given as:

$$M_{Rd} = A_{s1}f_{yd1}(d - x/2) + A_{s,T}kf_{y,T,e}d'' \quad (9)$$

Replacing $x$ and $A_{S,T}$ with Eq. (7), and Eq. (8) respectively, the $M_{RD}$ can be written as:

$$M_{Rd} = A_{s1}f_{yd1}\left(d - \frac{A_{s1}f_{yd1}+A_{s,T}kf_{y,T,e}}{2f_{cd1}\cdot b}\right) + \gamma \cdot n \cdot A_{fli} \cdot kf_{y,T,e}d'' \quad (10)$$

Based on the previous studies of FRP sheet strengthened RC beams, the maximum strain of FRP materials was usually considered as 70%-90% of their ultimate strain, such as the one in ACI equation [65], when the failure of the beams is not due to the rupture of FRP sheet. In this study, the failures of all beams were due to the rupture of the textile fabric mesh layer, however, the rupture of the layer did not correspond to the maximum strength of the beams. The main reasons for the failure of the beams were considered as the debonding of the TRM layer and consequent large bending deformation of the strengthening layer. The latter could be caused by complicated flexural-shear-tension behavior in strengthened RC beam. Elsanadedy et al. [33] also reported that 70% of rupture strain was conservatively the maximum assumed strain of the TRM debonding strain as long as the TRM layers with a good anchorage at the end and a shear failure was precluded in the strengthened beams. Therefore, the ratio of the calculative strain of textile fabric mesh layer corresponding to maximum flexural strength in the TRM-strengthened RC beams was assumed as about 60% to 70% of the yield strain of textile mesh materials, as the level for calculating of the load-carrying capacity of the beams.

Fig.13 compares the experimental results and the prediction results based on equation (10) with different assumed maximum strain ratio of textile mesh materials in the TRM layers and the enhancement ratio of the area of textile mesh considering the effect of textile reinforcement at different directions. Results show that the model presents a good agreement with the experimental results when the enhancement ratio and

maximum strain ratio are taken as 1.3 and 0.6, respectively, which both can be proved by the analyses described above in the study.

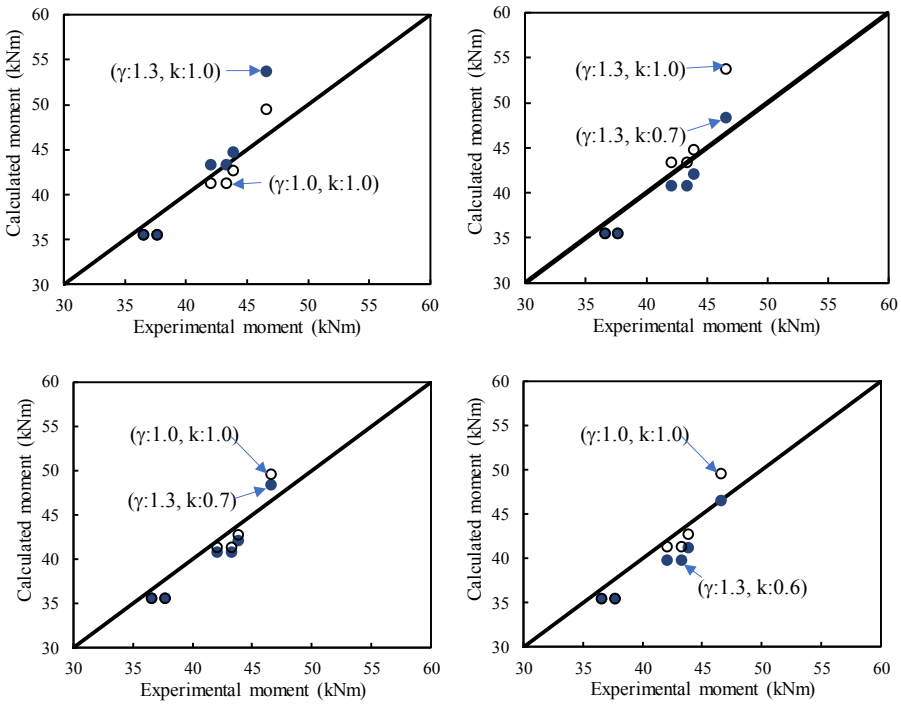


Fig.13 Comparison between modified *fib* model and experimental results

***(2) A simple modified model based on current AIJ code***

AIJ standard [66] also suggested a simplified calculation model for predicting the flexural moment of RC beams, which considered that the capacity could be calculated as a permissible moment capacity of RC beams when the tensile reinforcement ratio of the beams is less than a balanced rebar ratio. Referring to the definition of the related parameters plotted in Fig.14, the equation is given by:

$$M = a_t f_t j \qquad (11)$$

*where,* $j = (7/8)d$.

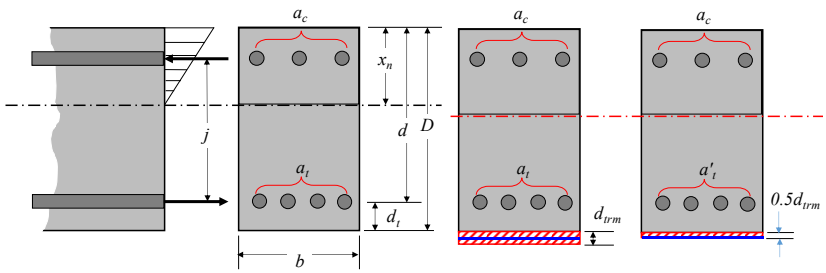

Fig.14 Sectional details in AIJ code and proposal for the modifications of TRM-strengthened RC beams

In this study, considering the strengthening effectiveness of TRM layer, the moment capacity of the RC beams is modified as:

$$M = a_t f_t j + A_{s,T} k f_{y,T} (D + 0.5 d_{trm}) \quad (12)$$

where $k$ is a key reduction factor of tensile stress of textile mesh to its yield stress at the ultimate state.

In this equation, several proposals were suggested for the factors $j$ and $k$ for a simplified modifying of the original AIJ model. Referring to AIJ code, the factor $j$ could be taken simply as 7d/8 or 6d/8, while $k$ could be assumed as 0.5 or 0.6 referring to previous research [67], respectively. Fig.15 compares the prediction results based on the modified model with the experimental results in the study. Results show that taking $j$ as 6d/8 is more reasonable for TRM-strengthened beams than other options, and there were not many differences between the cases when $k$ was taken as 0.5 or 0.6. This value is also near to the distance of the neutral axis to the compression edge of the beams reported before in the study. Considering this, the study suggests taking the factor $\boldsymbol{j}$ as 6d/8 to predict the moment capacity of TRM-strengthened RC beams.

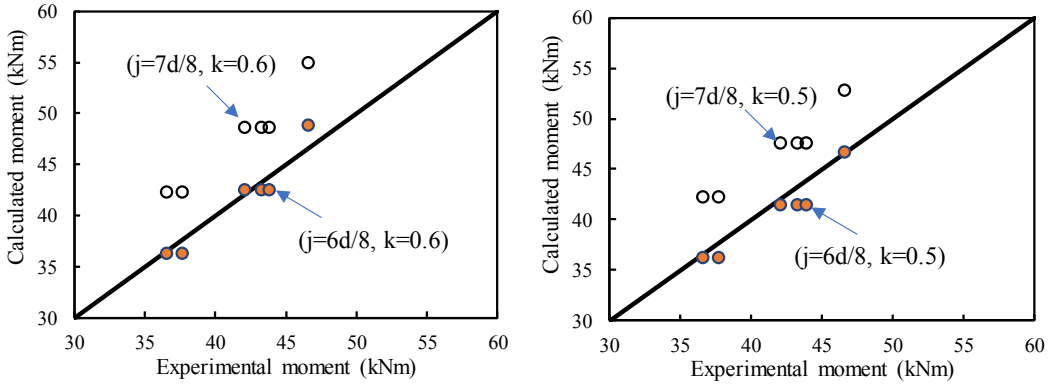


Fig.15 Comparisons between experimental results and modified AIJ equations with different factors

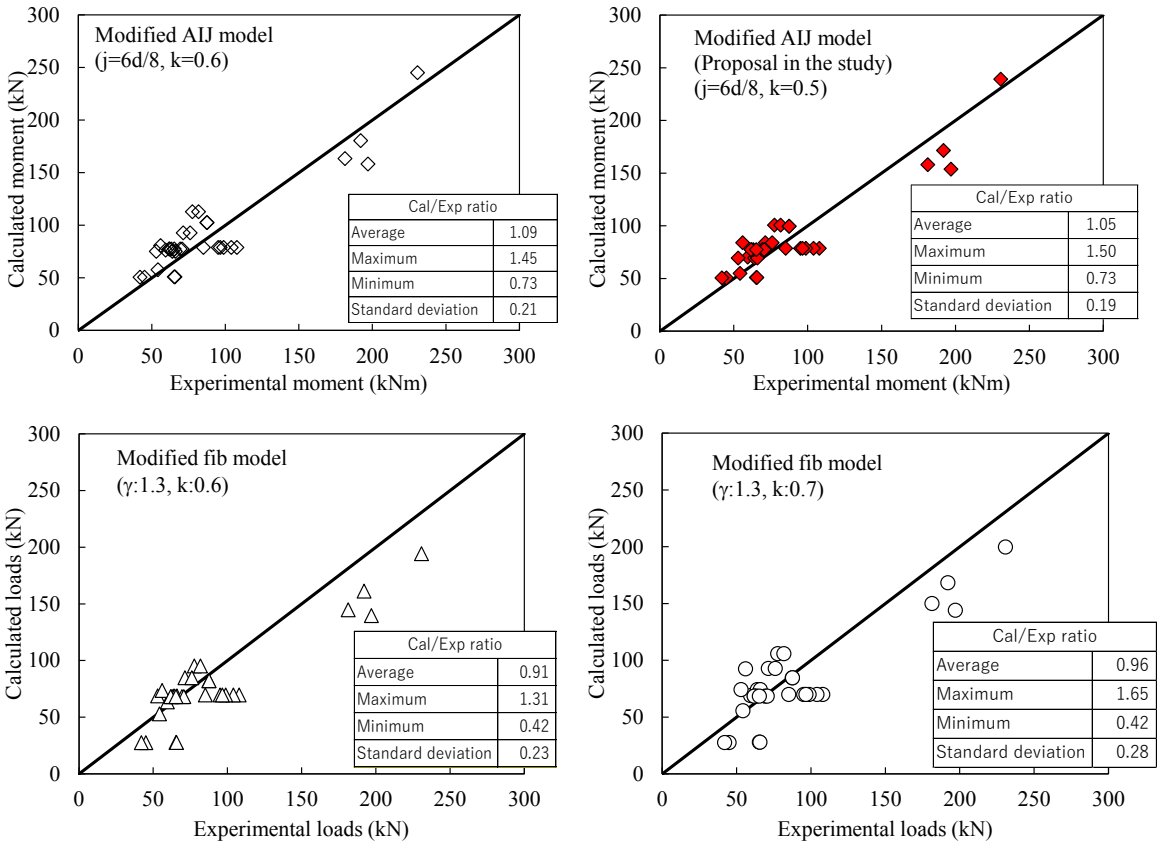


**Fig.16** Verification of the models

Fig.16 verifies the reliability and accuracy of the proposed model by comparing with the test resutls from the previous studies conducted by Ombres [24], Elsanadedy et al. [33], D' Ambrisi and Focacci [61], Loreto et al. [69], and Babaeidarabad et al. [70]. Comparing with other models, the proposed model presents the best accuracy of calculated load-experimental load ratio with a small standard deviation value. It should be noticed that the actual area of the fiber rovings in textile fabric mesh was used for all the calculations of the capacity in the study.

**(3) A simplified proposal for predicting capacity curves of TRM-strengthened RC beams**

Given the section stiffnesses ($S_i$) of RC beams strengthened TRC or TRM layer, as shown in Fig. 17, the midspan displacement of the beams under four-point flexural at the different stages (I~IV) can be calculated. The calculation model is expressed as,

$$u_i = \frac{M(3L^2 - 4a^2)}{24S_i} = \frac{Pa(3L^2 - 4a^2)}{48S_i} \quad (13)$$

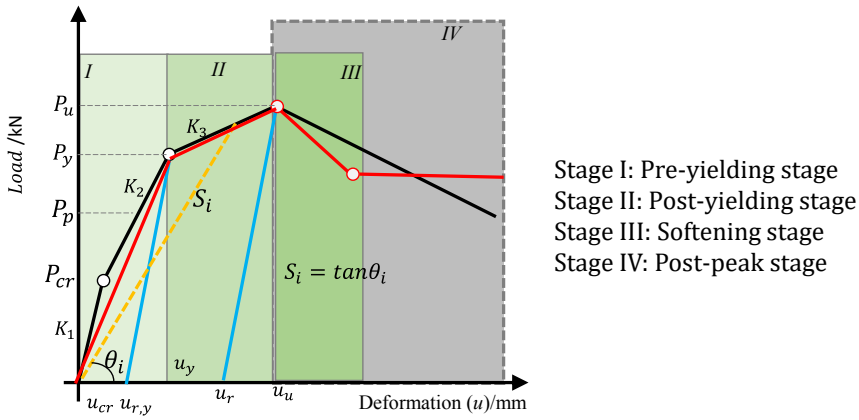


**Fig.17** Diagram of the proposal for evaluating of load-deformation of TRM-strengthened RC beams

Referring to FRP-strengthened RC beams [68], the section stiffness at the yield point and peak point of RC beams strengthened by TRC/TRM layers are written as

$$S_{yield} = \frac{E_s A_s d'^2}{\frac{\varphi_s}{n_{TRC}} + 0.013 + 10.5\alpha_{E,s}\rho_s} \tag{14}$$

$$S_{Peak} = \frac{E_{TRC} A_{TRC} d''^2}{\frac{\varphi_{TRC}}{a_2 n_{TRC}} + 0.0081 + 9.42\alpha_{E,f}\rho_{TRC}} \tag{15}$$

For the ratio of the modulus of steel and TRC/TRM materials to the elastic modulus of concrete, they are expressed as,

$$\alpha_{E,s} = \frac{E_s}{E_c};\ \alpha_{E,TRC} = \frac{E_{TRC}}{E_c} \tag{16}$$

where, $\rho_s = \frac{A_s}{bd'}$ , $\rho_s = \frac{A_{TRC}}{bd'}$.

Besides, the factors of the ratio of total moment of the beams to the contribution of steel bars ($a_1$) and to that of TRC materials ($a_2$) are presented as,

$$a_1 = \frac{M_s + M_{TRC}}{M_s} = 1 + 1.15\frac{E_{TRC}A_{TRC}}{E_s A_s}\left(\frac{d''}{d'}\right)^2 \tag{17}$$

$$a_2 = \frac{M_s + M_{TRC}}{M_{TRC}} = 1 + \frac{f_y A_s \eta_s d'}{\sigma_{TRC} A_{TRC} \eta_{TRC} d''} \tag{18}$$

Considering the coefficients of stress unevenness of steel rebars and FRP fabric mesh materials in TRC/TRM layers, the factors $\varphi_s$ and $\varphi_{TRC}$ are considered as identical. Therefore, referring to the literature [10, 68], the two factors in the study can be calculated as,

$$\varphi_s = \varphi_{TRC} = 1 - \frac{0.65 f_t}{a_1 \rho_{s,te} \sigma_s} \tag{19}$$

In the equations, $\rho_{s,te}$ is the ratio of the area of longitudinal steel rebars to the effective tensile area of concrete, simply being taken as 50% of the cross-section area of the beams. Therefore, $\rho_{s,te}$ was expressed as

$$\rho_{s,te} = \frac{A_s}{0.5bd'} \tag{20}$$

For the stress of steel rebars in RC beams, according to the literature, the internal arm coefficient of steel rebars ($\eta_s$) and TRC/TRM materials ($\eta_{TRC}$) both could be taken as 0.87 before yielding of and as 0.95 after the yielding of the beams. Therefore, the values of the stress of the steel rebars and TRC/TRM materials are calculated as,

$$\sigma_s = \frac{M}{a_1 \eta_s d' A_s} \tag{21}$$

$$\sigma_{TRC} = \frac{M - f_y A_s \eta_s d'}{\eta_{TRC} d'' A_{TRC}} \tag{22}$$

Applying the models proposed above, the midspan deflection of TRM-strengthened RC beams can be calculated. Fig.18 presents the comparison between the calculations based on proposed models and the experimental results of yield and peak midspan deflection. Results show that the proposal evaluates the experimental yield and peak midspan deflections of the beams with great accuracy both presenting a calculation error of less than about 10%.

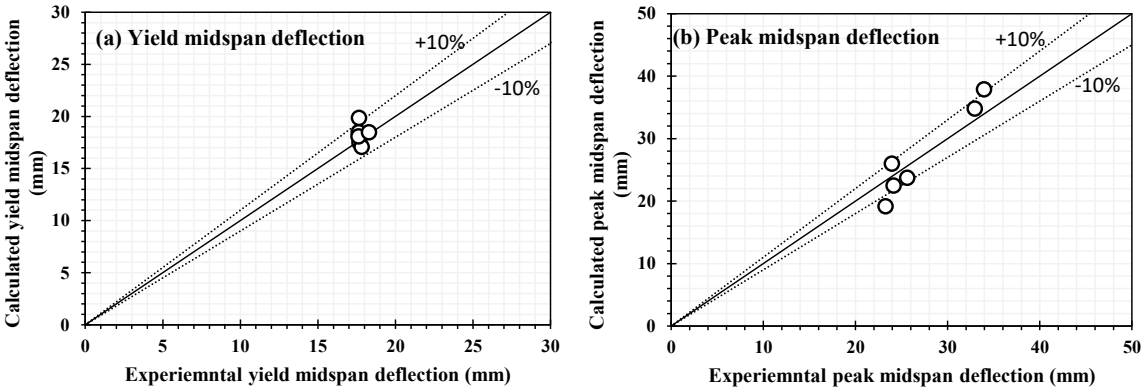


Fig.18 Comparison between calculated and experimental deflections at yield and peak states

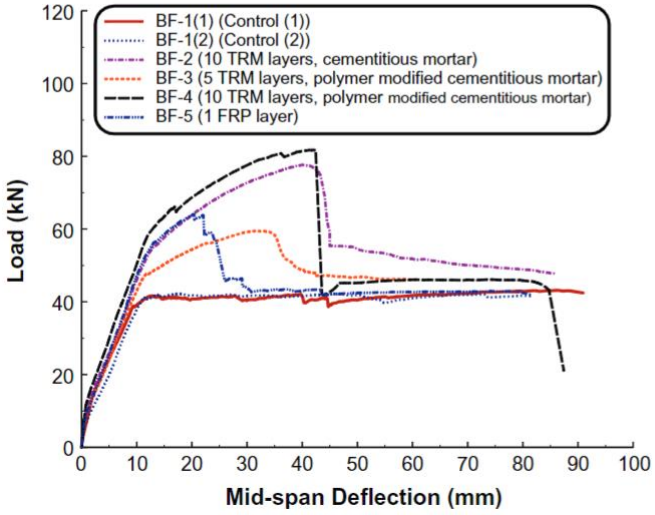


Fig.19 Load-deflection curves of test beams under monotonic flexural load [33]

About the softening stage of the TRM strengthened beams, previous research proved that the stage of RC beams under monotonic load was quite short shown in Fig.19, although the control beams in Ref. [33] had a typical flexural failure mode and their peak deformation were improved significantly after using TRM layer. In the study, however, the beams were subjected to cyclic loads and presented different softening behavior, in which the deformation corresponding to the 85% of peak load was about 3.0-5.0 times that at peak load. Therefore, referring to the beams in the literature and the data of the current research, the softening behavior of TRC/TRM retrofitted RC beams ($S$) can be expressed as a simplified function considering main factors including the number of layers of textile mesh ($N$), the mechanical properties of mortar/concrete in TRC/TRM (M) and flexural load type ($L$).

$$S = f(N, M, L) \tag{23}$$

In this study, to simplify the calculation, the midspan deflections of TRM-strengthened RC beams at 85% of peak load were taken as 3.0 times the deflections of the beams corresponding to their peak load. Therefore, using the proposed model, Eq. (12) ($j$:6d/8 and $k$:0.5), to predict the peak moment and assuming 90% of the peaking moment as the yielding moment of the TRM-strengthened beams, using the proposed models (Eqs.13-22) for the various deflections, the simplified model capacity curves of the beams can be established. The prediction results are plotted in Fig.20. Results show that the simplified capacity model can evaluate the experimental curves with a good agreement. However, it should be noticed that the capacity model still needs to be examined by more experimental investigations in the future.

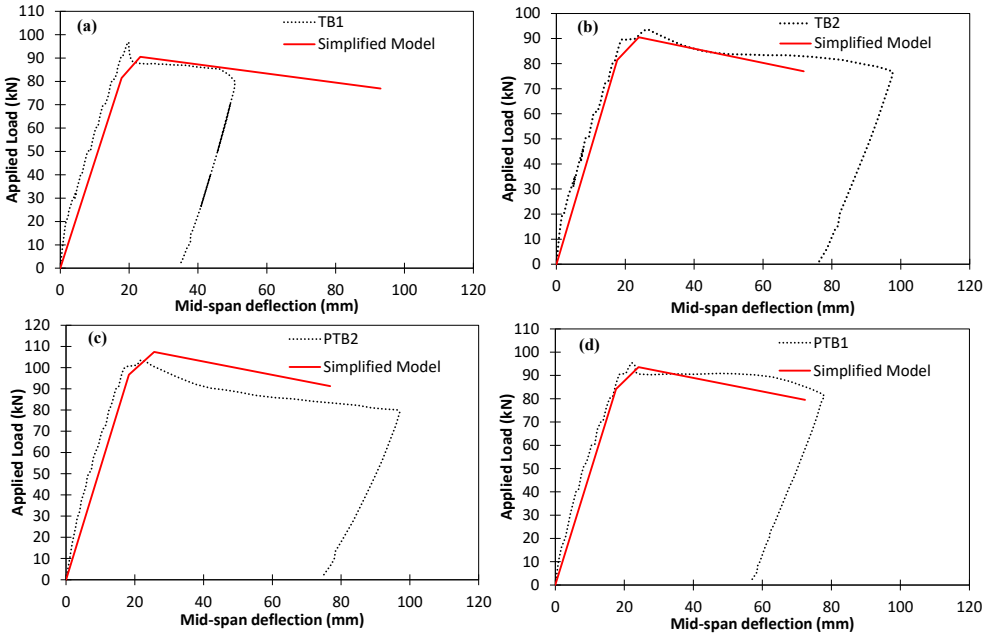


Fig.20 Comparison between model and experimental capacity curves

## 6 Concluding remarks

This paper experimentally investigated the cyclic flexural behavior of RC beams strengthened by a high-performance textile reinforced mortar layer. Based on the analyses and observations in the study, several simplified modifications were proposed for the calculation model of flexural capacity in fib methods and existing AIJ code. Based on the models, a simplified complete model was proposed to simulate the capacity curve of the TRM-strengthened RC beams. However, it should be noticed that the test matrixes adopted were limited in this study, more test studies are expected in the future to verify or modify the models. The

main findings of the preliminary study of TRM-strengthened RC beams under cyclic loads are summarized as:

(1). The strengthening effectiveness of the proposed high-performance TRM layer for RC beams under cyclic flexural loads was proved. The failure mode of the beams was affected by (a) the reinforcement ratio of original beams, (b) the interface bond between the strengthening layer and original beam, and (c) the number of the layers of textile meshes in the TRM layer. The debonding failure of TRM layer still could not be avoided at large deformation stage, however, the deflection of the beams corresponding to the debonding was significantly improved. Besides, the typical flexural cracks were developed fully in the TRM layer of the strengthened beams which may mean the TRM strengthening layer could co-work together with the original RC beams well based on the present preliminary study.

(2). The reinforcement ratio of original RC beams still was considered as a key factor affecting the flexural capacity and deformability of the TRM-strengthened RC beams. Based on the preliminary research with limited samples, the strengthening effectiveness of TRM layer for RC beams under cyclic loads may mainly depend upon the number of layers of textile fabric meshes compared with the mechanical properties of the mortar in TRM layer. However, more studies are required to validate this conclusion for the used mortars in the specimens all were compressive strength.

(3). Although the pre-cracking process did not significantly affect the load-carrying capacity of and deformation ability of TRM-strengthened RC beams, using this process presented a superiority in the reliability of TRM strengthening layer for RC beams under cyclic loads.

(4). With a proposed effective enhancement factor of the area of textile mesh and simply assuming the effective maximum strain of textile fabric mesh, this paper proposed several simplified modifications to predict the flexural capacity of TRM-strengthened RC beams based on *fib* model and AIJ code, which could evaluate the experimental results with good agreement. Using the above models and simplified proposals for the key various deflection of the beams, a simplified complete curve model was developed to evaluate the flexural capacity curves of TRM-strengthened RC beams which was proved with good accuracy.

**Acknowledgments**

The authors would like to thank the University of Leeds for the financial support and the contribution of Mr. G. Kampisios in conducting the experimental campaign as well as the technicians of the George Earl Heavy Structures Laboratory in the School of Civil Engineering.

**CRediT author statement**

**Gaochuang Cai:** Conceptualization, Methodology, Software, Data curation, Writing- Original draft preparation, Visualization, Investigation, Supervision. Writing- Reviewing and Editing. **Konstantinos Daniel Tsavdaridis**: Conceptualization, Methodology, Data curation, Visualization, Investigation, Supervision. **Amir Si Larbi1**: Data curation, Writing- Reviewing and Editing. **Phil Purnell**: Conceptualization, Methodology, Supervision.

**Conflict of Interest**

The authors declare that they have no conflict of interest.

**References**

[1]. Triantafillou, T., Deskovic, N. and Deuring, M. Strengthening of concrete structures with prestressed fiber reinforced plastic sheets. *ACI structural Journal* 89.3 (1992): 235-244.

[2]. Triantafillou, T. and Antonopoulos C. P. Design of concrete flexural members strengthened in shear with FRP. *Journal of composites for construction* 4.4 (2000): 198-205.

[3]. Wu, Zhishen, and Jun Yin. Fracturing behaviors of FRP-strengthened concrete structures. *Engineering Fracture Mechanics* 70.10 (2003): 1339-1355.

[4]. Teng, J. G., Chen, J. F., Smith, S. T., and Lam, L. FRP: strengthened RC structures. *Frontiers in Physics*, 2002.

[5]. Buyukozturk, O., Gunes, O., and Karaca, E.. Progress on understanding debonding problems in reinforced concrete and steel members strengthened using FRP composites." *Construction and Building Materials* 18.1(2004), 9-19.

[6]. Chen, L.,and Ozbakkaloglu, T.. Corner strengthening of square and rectangular concrete-filled FRP tubes. *Engineering Structures*, *117*(2016), 486-495.

[7]. Attari, N., Youcef, Y. S., and Amziane, S. Seismic performance of reinforced concrete beam–column joint strengthening by FRP sheets. In *Structures*. 20(2019) 353-364.

[8]. Hawileh, R. A., Musto, H. A., Abdalla, J. A., and Naser, M. Z. Finite element modeling of reinforced concrete beams externally strengthened in flexure with side-bonded FRP laminates. *Composites Part B: Engineering* (2019), 106952.

[9]. Cho, C. G., Han, B. C., Lim, S. C., Morii, N., and Kim, J. W. Strengthening of reinforced concrete columns by high-performance fiber-reinforced cementitious composite (HPFRC) sprayed mortar with strengthening bars. *Composite Structures. 202* (2018),1078-1086.

[10]. Zhang P, Zhu H, Meng SP, et al. Calculation of sectional stiffness and deflection of FRP sheets strengthened reinforced concrete beams. J Build Struct, 32(2011)87–94. (in Chinese)

[11]. Dehghani, A., Nateghi-Alahi, F., and Fischer, G. Engineered cementitious composites for strengthening masonry infilled reinforced concrete frames. *Engineering Structures*, *105*(2015), 197-208.

[12]. Al-Saadi, N. T. K., Mohammed, A., and Al-Mahaidi, R. Fatigue performance of NSM CFRP strips embedded in concrete using innovative high-strength self-compacting cementitious adhesive (IHSSC-CA) made with graphene oxide. *Composite Structures*, *163* (2017), 44-62.

[13]. Kang, S. B., Tan, K. H., Zhou, X. H., and Yang, B. Influence of reinforcement ratio on tension stiffening of reinforced engineered cementitious composites. *Engineering Structures*, *141*(2017), 251-262.

[14]. Deng, M., Dong, Z., and Ma, P. Cyclic loading tests of flexural-failure dominant URM walls strengthened with engineered cementitious composite. *Engineering Structures*, *194* (2019), 173-182.

[15]. Tariq, H., Jampole, E. A., and Bandelt, M. J. Fiber-hinge modeling of engineered cementitious composite flexural members under large deformations. *Engineering Structures*, *182*(2019), 62-78.

[16]. Huang, B. T., Li, Q. H., Xu, S. L., and Zhou, B. Strengthening of reinforced concrete structure using sprayable fiber-reinforced cementitious composites with high ductility. *Composite Structures*, *220*(2019), 940-952.

[17]. Harajli, M. H. Strengthening of concrete beams by external prestressing. PCI journal, 38(6) (1993), 76-88.

[18]. Matthys, S., and Taerwe, L. Concrete slabs reinforced with FRP grids. II: Punching resistance. *Journal of Composites for Construction*, *4*(3) (2000), 154-161.

[19]. Meng, W., and Khayat, K. H. Experimental and numerical studies on flexural behavior of ultrahigh-performance concrete panels reinforced with embedded glass fiber-reinforced polymer grids. Transportation Research Record, 2592(1) (2016), 38-44.

[20]. Tetta, Z. C., Koutas, L. N., and Bournas, D. A. Textile-reinforced mortar (TRM) versus fiber-reinforced polymers (FRP) in shear strengthening of concrete beams. *Composites Part B: Eng.*, *77* (2015), 338-348.

[21]. Raoof, S.M., Koutas, L.N. and Bournas, D.A. Textile-reinforced mortar (TRM) versus fibre-reinforced polymers (FRP) in flexural strengthening of RC beams. *Construction and Building Materials*, *151*(2017), pp.279-291.

[22]. Brückner, A., Ortlepp, R., and Curbach, M.. Anchoring of shear strengthening for T-beams made of textile reinforced concrete (TRC). *Materials and Structures*, *41*(2) (2008), 407-418.

[23]. Al-Salloum, Y. A., Elsanadedy, H. M., Alsayed, S. H., and Iqbal, R. A. Experimental and numerical study for the shear strengthening of reinforced concrete beams using textile-reinforced mortar. *Journal of Composites for Construction*, *16*(1) (2011), 74-90.

[24]. Ombres, L. Flexural analysis of reinforced concrete beams strengthened with a cement based high strength composite material. *Composite Structures,* 94(2011)**,** 143-155.

[25]. Verbruggen, S., Tysmans, T., & Wastiels, J. TRC or CFRP strengthening for reinforced concrete beams: An experimental study of the cracking behaviour. *Engineering structures*, *77*(2014), 49-56.

[26]. Tetta, Z. C., and Bournas, D. A. TRM vs FRP jacketing in shear strengthening of concrete members subjected to high temperatures. *Composites Part B: Engineering*, *106*(2016), 190-205.

[27]. Raoof, S. M., and Bournas, D. A. Bond between TRM versus FRP composites and concrete at high temperatures. *Composites Part B: Engineering*, *127*(2017), 150-165.

[28]. Scheerer, S., Zobel, R., Müller, E., Senckpiel-Peters, T., Schmidt, A., and Curbach, M. Flexural Strengthening of RC Structures with TRC—Experimental Observations, Design Approach and Application. *Applied Sciences*, *9*(7) (2019), 1322.

[29]. Hu, X. Q., Yin, S., and Lv, H. L. Eccentric compression behavior of TRC-strengthened concrete columns under chloride environment. *Anti-Corrosion Methods and Materials*, *66*(2) (2019), 159-167.

[30]. Ortlepp, R., Hampel, U. and Curbach, M. A new approach for evaluating bond capacity of TRC strengthening. Cement and Concrete Composites, 28(2006), 589-597.

[31]. Schladitz, F., Frenzel, M., Ehlig, D. and Curbach, M. Bending load capacity of reinforced concrete slabs strengthened with textile reinforced concrete. Engineering Structures, 40(2012), 317-326.

[32]. Si Larbi, A., Contamine, R. and Hamelin, P. TRC and hybrid solutions for repairing and/or strengthening reinforced concrete beams. Engineering Structures, 45(2012), 12-20.

[33]. Elsanadedy, H. M., Almusallam, T. H., Alsayed, S. H., and Al-Salloum, Y. A. Flexural strengthening of RC beams using textile reinforced mortar–Experimental and numerical study. *Composite Structures*, *97*(2013), 40-55.

[34]. Yin, S., Xu, S., and Lv, H. Flexural Behavior of Reinforced Concrete Beams with TRC Tension Zone Cover. Journal of Materials in Civil Engineering, 26(2014), 320-330.

[35]. Larbi, A. S., Contamine, R., Ferrier, E., & Hamelin, P. (2010). Shear strengthening of RC beams with textile reinforced concrete (TRC) plate. Construction and Building Materials, 24(10), 1928-1936.

[36]. Tzoura, E., & Triantafillou, T. C. (2016). Shear strengthening of reinforced concrete T-beams under cyclic loading with TRM or FRP jackets. *Materials and Structures*, *49*(1-2), 17-28.

[37]. Contamine, R., Larbi, A. S., & Hamelin, P. (2013). Identifying the contributing mechanisms of textile reinforced concrete (TRC) in the case of shear repairing damaged and reinforced concrete beams. *Engineering Structures,* 46, 447-458.

[38]. Al-Salloum, Y. A., Elsanadedy, H. M., Alsayed, S. H., & Iqbal, R. A. (2012). Experimental and numerical study for the shear strengthening of reinforced concrete beams using textile-reinforced mortar. Journal of Composites for Construction, 16(1), 74-90.

[39]. Yin, S., Xu, S., & Lv, H. (2014). Flexural behavior of reinforced concrete beams with TRC tension zone cover. *Journal of Materials in Civil Engineering*, *26*(2), 320-330.

[40]. Scheerer, S., Zobel, R., Müller, E., Senckpiel-Peters, T., Schmidt, A., & Curbach, M. (2019). Flexural strengthening of RC structures with TRC—Experimental observations, design approach and application. *Applied Sciences*, *9*(7), 1322.

[41]. Ombres, L. (2011). Flexural analysis of reinforced concrete beams strengthened with a cement based high strength composite material. *Composite Structures*, *94*(1), 143-155.

[42]. Al-Lami, K., & D'Antino, T. (2020). Durability of Fabric-Reinforced Cementitious Matrix (FRCM) Composites: A Review. Applied Sciences, 10(5), 1714.

[43]. Koutas, L. N., Tetta, Z., Bournas, D. A., & Triantafillou, T. C. (2019). Strengthening of concrete structures with textile reinforced mortars: state-of-the-art review (Doctoral dissertation, American Society of Civil Engineers).

[44]. Cai, G., Tsavdaridis, K. D., Yoshizawa, M., and Purnell, P. Flexural behaviors of high performance TRM-retrofitted RC beams under cyclic loading, *Proc. Japan concrete institute*, Sapporo, 2019.07

[45]. Cai, G., Tsavdaridis, K. D., Purnell, P. and Yoshizawa, M. Deformation and strengthening effectiveness of high performance TRM for RC beams under cyclic loading: sectional analysis and deformation capacity, 3rd ACF Symposium on "Assessment and Intervention of Existing Structures", 2019, Sapporo, Japan

[46]. CEN (European Committee for Standardization) EN 1992-1-1: Eurocode 2: Design of concrete structures. Part 1-1: General rules and rules for buildings. CEN, Brussels, 2004

[47]. Hussain, M., Sharif, A., Basunbul, I., Baluch, M. and Al-Sulaimani, G. Flexural behavior of precracked reinforced concrete beams strengthened externally by steel plates. ACI Structural Journal, 92 (1995), 14-22.

[48]. Marco, A. and Antonio, N. Behavior of Precracked RC beams strengthened with Carbon FRP sheets. 1997.

[49]. Benjeddou, O., Ouezdou, M. B., and Bedday, A. Damaged RC beams repaired by bonding of CFRP laminates. Construction and building materials, 21(2007), 1301-1310.

[50]. Dias, S. J. E., and Barros, J. A. O. NSM shear strengthening technique with CFRP laminates applied in high-strength concrete beams with or without pre-cracking. Composites Part B: Engineering, 43(2012), 290-301.

[51]. American Concrete Institute (ACI).ACI 437.1R, Load Tests of Concrete Structures: Methods, Magnitude, Protocols and Acceptance Criteria. ACI, USA. 2007.

[52]. FEMA-461. Interim Testing Protocols for Determining the Seismic Performance Characteristics of Structural and Nonstructural Components. In: FEMA-461 (ed.). 2007

[53]. Ridge, A. R. and Ziehl, P. H. Evaluation of strengthened reinforced concrete beams: cyclic load test and acoustic emission methods. ACI Structural Journal, 103(2006), 832.

[54]. Galati, N., Nanni, A., Gustavo T. J. and Zizehl, P. H. In-situ evaluation of two concrete slab systems. I: Load determination and loading procedure. Journal of Performance of Constructed Facilities, 22(2006), 207-216.

[55]. Liu, Z. and Ziehl, P. H. Evaluation of reinforced concrete beam specimens with acoustic emission and cyclic load test methods. ACI Structural Journal, 106(2009), 288.

[56]. Dong, J., Wang, Q., and Guan, Z. Structural behaviour of RC beams externally strengthened with FRP sheets under fatigue and monotonic loading. Engineering Structures, 41(2012), 24-33.

[57]. Barrios, F., and Ziehl, P. H. Cyclic load testing for integrity evaluation of prestressed concrete girders. ACI Structural Journal-American Concrete Institute, 109(2012), 615.

[58]. Elbatanouny, M. K., Nanni, A., Ziehl, P. H. and Matta, F. Condition Assessment of Prestressed Concrete Beams Using Cyclic and Monotonic Load Tests. ACI Structural Journal, 112(2015), 81.

[59]. Lam, L., Teng, J. G., Cheung, C. H., and Xiao, Y. FRP-confined concrete under axial cyclic compression. *Cement and Concrete composites*, *28*(10) (2006) 949-958.

[60]. Wang, J. H., Cai, G., and Wu, Q. Basic mechanical behaviours and deterioration mechanism of RC beams under chloride-sulphate environment. *Construction and Building Materials*, *160* (2018) 450-461.

[61]. D'Ambrisi, A., and Focacci, F. Flexural strengthening of RC beams with cement-based composites. *Journal of Composites for Construction*, *15*(5) (2011)707-720.

[62]. Regan P. Basic design for moment, shear and torsion. In: fib Bulletin 52 (Structural Concrete – Textbook on behaviour, design and performance, vol. 2, section 4.4.1 pp. 171–249), Lausanne, 2010.

[63]. Müller G.S., Haist M. Concrete. In: fib Bulletin 52 (Structural Concrete – Textbook on behaviour, design and performance, vol. 2, section 3.1, pp. 35-149.), Lausanne, 2010

[64]. Fédération Internationale du Béton (*fib*), Model Code 2010 - Final draft, Vol. 1, fédération internationale du béton, Bulletin 65, Lausanne, Switzerland, Vol. 2, 2012.

[65]. American Concrete Institute (ACI). ACI Committee 440. State of the art report on fiber reinforced plastic reinforcement for concrete structures. Detroit (Michigan, USA): American Concrete Institute (ACI); 1996.

[66]. Architectural Institute of Japan, AIJ standard for structural calculation of reinforced concrete structures, Tokyo. Japan, 2010. (in Japanese)

[67]. Bui, T.L., Larbi, A.S., Reboul, N. and Ferrier, E., Shear behaviour of masonry walls strengthened by external bonded FRP and TRC. *Composite Structures*, *132*(2015)923-932.

[68]. Dong, Z., Zhang, P., Zhu, H., Wu, G., & Wu, Z. Study on stiffness and recoverability of Fiber Reinforced Polymers-Reinforced Concrete (FRP-RC) composite T-beams with prefabricated Basalt fiber-reinforced polymers shell. Journal of Reinforced Plastics and Composites, 35(6) (2015)516–529.

[69]. Loreto, G., Leardini, L., Arboleda, D., & Nanni, A. Performance of RC slab-type elements strengthened with fabric-reinforced cementitious-matrix composites. *Journal of Composites for Construction*, *18*(3) (2014), A4013003.

[70]. Babaeidarabad, S., Loreto, G., & Nanni, A. Flexural strengthening of RC beams with an externally bonded fabric-reinforced cementitious matrix. *Journal of Composites for Construction*, *18*(5) (2014) 04014009.